Appl. Phys. B 68, 349–353 (1999)

Applied Physics B
Lasers
and Optics

Enhancing the yield in surface sum-frequency generation by the use of surface polaritons

E.R. Eliel, E.W.M. van der Ham*, Q.H.F. Vrehen

Huygens Laboratory, Leiden University, P.O. Box 9504, 2300 RA Leiden, The Netherlands
(Fax:+31-71/527-5819, E-mail: eliel@molphys.leidenuniv.nl)

Received: 23 December 1998

Abstract. The efficiency of sum-frequency generation at an air–metal interface can be enormously increased by coupling one of the input waves into a surface polariton. Experimental results for various configurations of input beams and couplers are discussed.

PACS: 42.65.Ky; 41.60.Cr; 73.20.M

Over the last ten years sum-frequency (SF) generation has developed into a standard tool for the study of surfaces and interfaces that are covered by molecular monolayers [1–4]. The vast majority of studies pertain to the wavelength range $\lambda < 10\,\mu$m because of the ready availability of powerful tunable infrared sources at these wavelengths. The application of free-electron lasers to the field of sum-frequency spectroscopy has brought about a fundamental change here because these lasers are tunable over very wide wavelength ranges and reach into the far-IR [5–11]. Since SF studies with FELs are nontrivial from an experimental point of view, the use of table-top IR sources, even when they are somewhat less powerful, remains very appealing.

In SF studies of monolayers, the flux of generated photons is quite small. On the one hand this is because nonlinear optical processes like SF generation are highly inefficient, on the other because the sample has essentially zero depth. In view of the signal-to-noise ratio it is then important to investigate methods to maximize the signal yield given the output power of the required visible and tunable IR laser sources.

In theory the SF generation process can be made more efficient by increasing the flux density of the primary radiation. Given the output power of the sources, this can be implemented by reducing the spot size of *both* beams. Sample damage sets a limit to this approach. However, if only one of the beams is close to damage threshold there is another option: to employ field-enhancement techniques for the other input frequency. This will lead to a larger SF yield since one of the driving fields is enhanced. Enhancement of the field at the interface of two media occurs for instance in a total-internal-reflection (TIR) geometry just beyond the angle for total internal reflection, or when one excites a surface polariton at the interface [12]. Both these methods have been successfully employed in nonlinear optical experiments [13–17]. Whereas the TIR geometry is being applied in some instances to SFG from adsorbed monolayers [14–17], the possibilities offered by the application of surface polaritons to SFG of interfacial layers have remained unexplored until recently. In this article we summarize the results of our recent studies on the application of surface polaritons to sum-frequency generation at interfaces [18–20].

1 Surface plasmon polaritons

The possibility that electromagnetic waves can propagate on a surface or interface was first discussed by Sommerfeld in the context of the propagation of radio waves [21]. These solutions to Maxwell's equations exist under well-defined conditions regarding the complex dielectric functions $\varepsilon_a(\omega) = \varepsilon'_a(\omega) + \imath\varepsilon''_a(\omega)$ and $\varepsilon_b(\omega) = \varepsilon'_b(\omega) + \imath\varepsilon''_b(\omega)$ of the media above ($z > 0$) and below ($z < 0$) the interface, respectively; either $\varepsilon'_a(\omega) < 0$ and $\left|\varepsilon'_a(\omega)\right| > \varepsilon'_b(\omega)$ or $\varepsilon'_b(\omega) < 0$ and $\left|\varepsilon'_b(\omega)\right| > \varepsilon'_a(\omega)$. The electric field is p-polarized and can be written as

$$\mathbf{E}^a(\omega) = \left(E^a_x(\omega)\mathbf{x} + E^a_z(\omega)\mathbf{z}\right) \exp\left[-\alpha^\omega_a z - \imath\omega t + \imath K^\omega_{\mathrm{SPP}} x\right] , \tag{1}$$

$$\mathbf{E}^b(\omega) = \left(E^b_x(\omega)\mathbf{x} + E^b_z(\omega)\mathbf{z}\right) \exp\left[-\alpha^\omega_b z - \imath\omega t + \imath K^\omega_{\mathrm{SPP}} x\right] , \tag{2}$$

where the surface excitation propagates along the x direction. Because of the continuity of the tangential component of the electric field and the normal component of the displacement field one has $E^a_x(\omega) = E^b_x(\omega)$ and $E^a_z(\omega) = (\varepsilon_b(\omega)/\varepsilon_a(\omega))\, E^b_z(\omega)$. On both sides of the interface the amplitude of the wave decays away from the interface with the

---
* *Present address*: NMI, P.O. Box 654, 2600 AR Delft, The Netherlands

transverse damping constant

$$\alpha_{\mathrm{i}}^{\omega} = \sqrt{\left(K_{\mathrm{SPP}}^{\omega}\right)^2 - \varepsilon_i(\omega)\left(\frac{\omega}{c}\right)^2}\,, \quad i \in (a, b)\,. \tag{3}$$

The (complex) propagation constant of the surface wave is given by

$$K_{\mathrm{SPP}}^{\omega} \equiv K^{\omega} + \imath\kappa^{\omega} = \frac{\omega}{c}\sqrt{\frac{\varepsilon_a(\omega)\varepsilon_b(\omega)}{\varepsilon_a(\omega)+\varepsilon_b(\omega)}}\,, \tag{4}$$

with $K^{\omega} > \omega/c$.

In the present case we employ surface waves propagating along the interface between vacuum and a metal; these waves are commonly called surface plasmon polaritons (SPPs). Our studies are limited to frequencies well below the metal's plasma frequency. Hence $\varepsilon_a(\omega) = 1$ and $\varepsilon_b'(\omega) < 0$ with $\left|\varepsilon_b'(\omega)\right| > \varepsilon_a(\omega)$. In the low-frequency limit $(\omega \to 0)$ these waves are also called surface electromagnetic waves (SEWs) emphasizing the fact that, in this limit, the coupling with the electronic system is weak.

The dispersion relation of a SPP along an air–metal interface is shown in Fig. 1 (solid curve) together with that of electromagnetic radiation in free space (dashed curve). The figure directly shows the wave vector mismatch between an SPP and free-space radiation at the same frequency. Because of this mismatch some element is required to couple free-space radiation with a SPP at the air–metal interface.

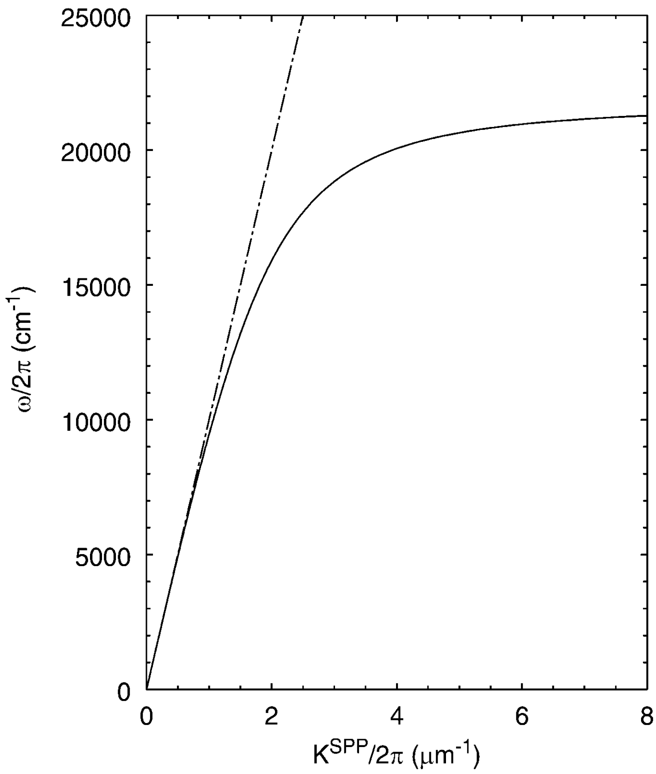

Fig. 1. Dispersion relation of a surface plasmon polariton propagating along the interface between vacuum and a metal (*solid curve*). The *dashed line* shows the dispersion relation of free-space electromagnetic radiation

2 Experimental method

The sum-frequency spectrometer used in the experiments described here is discussed in [9, 10]. Briefly, wavelength-tunable ($5 < \lambda_{\mathrm{ir}} < 110\,\mu$m) IR radiation from the FELIX free-electron laser [5] is mixed at the surface of a silver film with the output of a fixed-frequency ($\lambda_{\mathrm{vis}} = 523.5$ nm) visible laser system. Both lasers generate bursts ($\approx 5\,\mu$s long) of synchronized short, powerful pulses that overlap temporally and spatially on the sample. In the experiments described here FELIX delivers pulses of about 3 ps duration with an energy content of 2 μJ at a 1-GHz repetition rate, while the visible laser yields pulses of about 7 ps duration with an energy of 4 μJ at a repetition rate of 250 MHz. Both laser beams are *p*-polarized. The generated sum-frequency radiation is emitted as a collimated beam and is focussed on a liquid-N_2-cooled CCD camera that serves as a detector. A narrowband interference filter set with a compound transmission of approximately 50% at the sum frequency is used to suppress stray light at the visible input wavelength.

The effect of surface plasmon polaritons on the sum-frequency yield is most clearly observed when the SPP, be it at visible or IR frequencies, becomes resonantly excited. This is realized when the magnitude of the wave vector K^{ω} of the SPP at frequency ω matches $k_x(\omega)$, the component parallel to the interface of the wave vector of the incident radiation at that frequency. Because $K^{\omega} > k^{\omega} > k_x^{\omega}$, a coupler is required to realize the wave vector matching. Both gratings and prisms can be employed for this purpose.

3 Employing a SPP at the IR frequency

One of the attractive features of SPPs at IR frequencies ($\nu \approx 1000\,\mathrm{cm}^{-1}$) is that the longitudinal damping length $(\kappa^{\mathrm{ir}})^{-1}$ of the SPP is macroscopically long (of the order of a few cm). It is then possible to spatially separate the SPP-coupling and SF-generation processes on the sample.

In the experiment we couple to the SPP via a grating that has a period $a = 5.24\,\mu$m. Wave vector matching in the $\lambda_{\mathrm{ir}} = 10\,\mu$m band is achieved on this grating when

$$K^{\mathrm{ir}} = k_x^{\mathrm{ir}} - \frac{2\pi}{a}\,, \tag{5}$$

where k_x^{ir} represents the component of the wave vector of the IR input radiation along the interface. The SEW then is counterdirectional to the IR input wave. Figure 2 shows the results for the sum-frequency yield for counter-directional input beams having angles of incidence of 55.5° for the IR, and 36° for the visible input beam [20]. At resonance, the SF yield is enhanced by a factor 35. Also shown in Fig. 2 is the measured efficiency of coupling the IR radiation into the surface wave (circles). The wavelength dependence of the two quantities is indeed very similar, suggesting that the surface–polariton coupling is responsible for the resonant increase of the SF yield.

Supplemental evidence for this inference comes from an experiment where there is no spatial overlap of the two input beams because the visible input beam no longer hits the grating. A SF signal is easily measured if the visible beam has overlap with the surface wave that propagates as a free

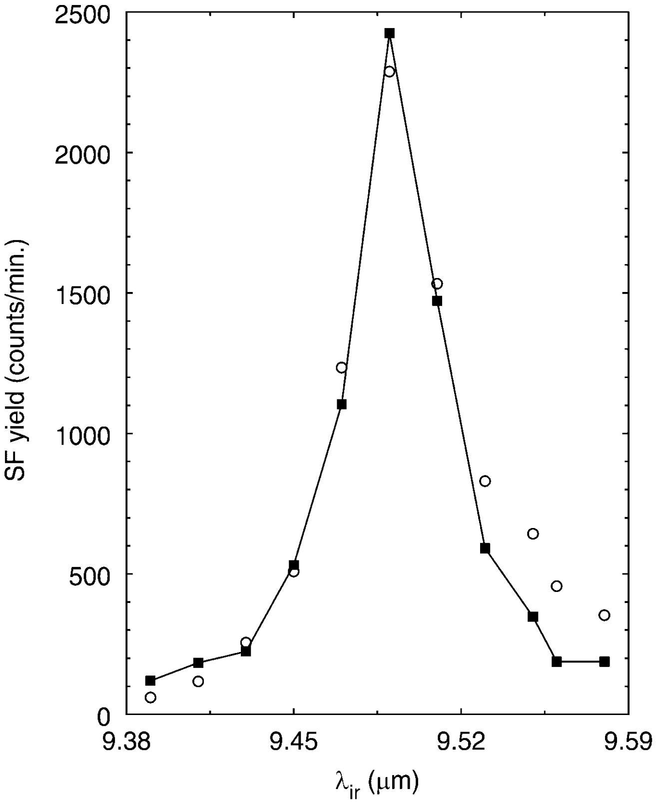

Fig. 2. Experimental results for the sum-frequency yield as a function of the IR wavelength (*solid circles*). Here the IR radiation is coupled into a surface electromagnetic wave along the silver–air interface. The *open symbols* show the measured excitation efficiency of the surface electromagnetic wave

wave along the interface. Indeed, with the visible beam just beyond the grating the SF yield is almost identical to the value obtained with the visible and IR beam overlapping on the grating. If the visible beam is displaced in the opposite direction the SF yield is zero; the SEW does not propagate in this direction.

For applications in spectroscopy the case under discussion is more of academic than of practical interest since the SPP resonance is so narrow ($\approx 4\,\mathrm{cm}^{-1}$ full width at half maximum). Its width is thus of the same order or smaller than that of the vibrational resonances of the adsorbed species. A spectroscopic experiment then becomes cumbersome, requiring simultaneous tuning of the IR wavelength and of the angle of incidence of the IR input beam.

4 Employing a SPP at the visible frequency

These problems do not arise when the fixed-frequency visible radiation is coupled into a SPP. The wave-vector-matching problem associated with the excitation of the polariton is then independent of the frequency of the IR radiation. Variation of the IR frequency will not affect the strength of the field at the interface associated with the SPP.

In the experiments described here we use both prism and grating couplers in configurations where the input beams run either counter- or co-directional. In the experiments involving prism coupling we employ a 90° fused-silica prism with a 50-nm-thick silver film on the hypotenuse. Wave vector matching at the air–silver interface is achieved by choosing the appropriate angle of incidence θ_{vis} of the visible input radiation:

$$K^{\mathrm{vis}} = n(\omega_{\mathrm{vis}})\frac{\omega_{\mathrm{vis}}}{c}\sin\theta_{\mathrm{vis}}\ , \tag{6}$$

where $n(\omega_{\mathrm{vis}})$ is the refractive index of fused silica at frequency ω_{vis}. The SPP is *co-directional* with the visible input beam. In the experiments involving grating coupling we employ a flat glass substrate containing the grating structure, the latter having a period $a = 301$ nm. The substrate is overcoated with a 200-nm-thick silver film. Wave vector matching at the air–silver interface is achieved when

$$K^{\mathrm{vis}} = \frac{\omega_{\mathrm{vis}}}{c}\sin\theta_{\mathrm{vis}} - \frac{2\pi}{a}\ . \tag{7}$$

Since $a < \lambda_{\mathrm{vis}}$ the SPP is *counter-directional* to the visible input beam.

Figure 3 shows the measured sum-frequency yield as a function of the angle of incidence of the visible input beam for counter-directional IR and visible input beams. The top frame displays the results for the prism coupler whereas the bottom frame shows those for the grating coupler. Most notable is the enormous difference in the yield enhancement:

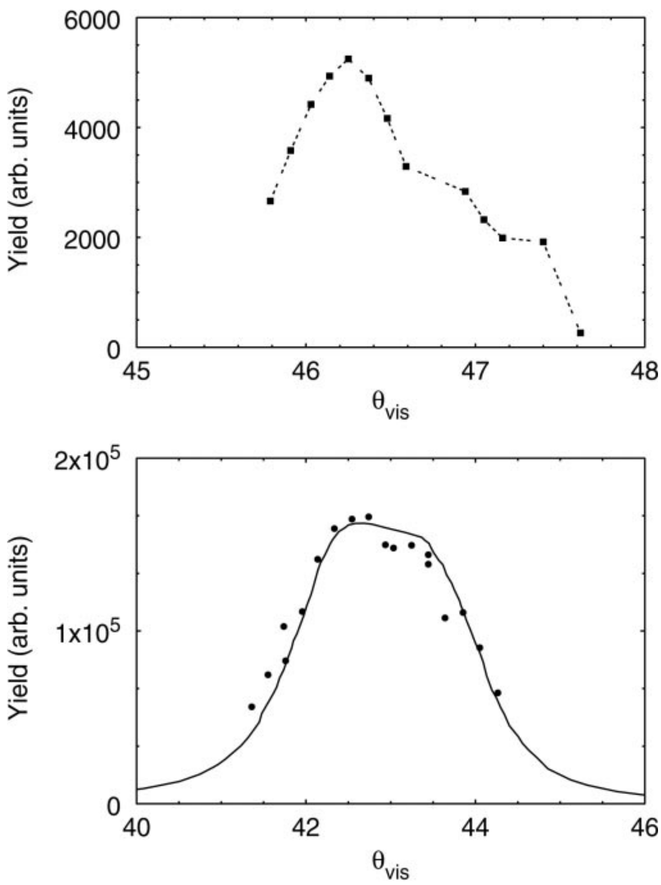

Fig. 3. Experimental results for the sum-frequency yield for the case that the visible input beam is coupled into a surface plasmon polariton. The *top frame* shows the results for a prism coupler while the *bottom frame* shows the results for a grating coupler. In both cases the input beams are counter-directional. The *solid line* in the *bottom frame* shows the calculated variation of the enhancement, scaled down by a factor 2.5 to fit the experimental results

while it is of order 100 for the prism coupler it is of order 10 000 for the grating coupler. As will be argued below, this large difference can be explained in terms of an additional enhancement that is mediated by the resonant excitation of a SPP at the sum frequency.

In order to understand this phenomenon we have to look at the spatial variation of the nonlinear polarization $\widetilde{\mathbf{P}}^{(2)}(\mathbf{r}, t)$ along the interface:

$$\widetilde{\mathbf{P}}^{(2)}(\mathbf{r}, t) = \mathbf{P}^{(2)}(\omega_{sfg})\delta(z) \exp\left[\imath k_x^{\mathrm{NL}}(\omega_{sfg})x - \imath\omega_{sfg}t\right] , \quad (8)$$

where $\mathbf{P}^{(2)}(\omega_{sfg})$ is the interfacial nonlinear surface polarization. For the situation shown in the bottom frame of Fig. 3 the visible polariton is co-diretional with the IR input beam; thus

$$k_x^{\mathrm{NL}}(\omega_{sfg}) = K^{\mathrm{vis}} + k_x(\omega_{\mathrm{ir}}) , \quad (9)$$

where $k_x(\omega_{\mathrm{ir}})$ is the component of the wave vector of the IR input radiation parallel to the interface. In the configuration at hand $|k_x^{\mathrm{NL}}(\omega_{sfg})| > \omega_{sfg}/c$; hence the nonlinear polarization cannot radiate into free space.

The nonlinear polarization at the sum-frequency can, however, itself excite a SPP; the latter becomes resonantly enhanced when its wave vector K^{sfg} matches $k_x^{\mathrm{NL}}(\omega_{sfg})$, the wave vector of the driving nonlinear polarization [13, 22]. In general, however, there is a mismatch $\Delta k(\omega_{sfg}) \equiv \left|K^{sfg} - k_x^{\mathrm{NL}}(\omega_{sfg})\right|$ between these wave vectors, setting a limit to the resonant enhancement.

The generation of a surface polariton at the sum frequency by the nonlinear surface polarization is very similar to SFG in the bulk or in waveguides for the case that the propagation vectors of the driving nonlinear polarization and of the generated field point in exactly the same direction. This situation gives rise to coherent build-up of the field at the sum frequency over a length equal to the coherence length,

$$\ell_{\mathrm{c}} \equiv \left[\left(\Delta k(\omega_{sfg})\right)^2 + \left(\kappa^{sfg}\right)^2\right]^{-\frac{1}{2}} . \quad (10)$$

Here $(\kappa^{sfg})^{-1}$ represents the longitudinal damping length of the surface polariton at the sum frequency.

The enhancement that one measures in the experiment is then due to a combination of a resonant increase of the field associated with the SPP at ω_{vis} AND a resonant buildup of the field associated with the SPP at ω_{sfg}. These two resonances do overlap but not perfectly. As a function of the angle of incidence of the visible beam the two resonances are separated by a full width, roughly.

This double enhancement does not play a role in the experiment with the prism coupler. In that case, since the visible polariton and IR input beam are counter-directional [compare with (9)]

$$k_x^{\mathrm{NL}}(\omega_{sfg}) = K^{\mathrm{vis}} - k_x(\omega_{\mathrm{ir}}) . \quad (11)$$

Because of the minus sign $\left|k_x^{\mathrm{NL}}(\omega_{sfg})\right| < n(\omega_{sfg})\omega_{sfg}/c$: when the visible input radiation resonates with a SPP the nonlinear polarization can directly radiate into the prism. A single enhancement factor thus comes into play in this case.

When the input beams are chosen to be *co-directional* the situation reverses. In that case the prism coupler gives the higher yield; the plus and minus signs in (9) and (11) are interchanged. With the prism coupler the nonlinear polarization at the sum frequency can only couple to a SPP, whereas with the grating coupler it can radiate into free space. Table 1 summarizes the experimental results for the peak value of the enhancement of the SF yield. The table suggests a certain symmetry in the yield: single and double enhancement of the yield is achievable with either grating or prism coupler. The difficulty of the experiment is, however, much smaller in the counterdirectional setup: the angular separation of the reflected visible input beam and of the generated SF radiation is considerable in contrast to the case of codirectional input beams.

Table 1. Summary of enhancement factors

	Co-directional	Counter-directional
Prism	10^4	10^2
Grating	10^2	10^4

5 Conclusions

It was shown that the sum-frequency flux from a metal–air interface can be enormously enhanced when one of the two input beams is coupled into a surface plasmon polariton. In various configurations, involving prism and grating couplers, we have achieved an increase of this flux by two to four orders of magnitude. The hundredfold increase of the flux can be explained in terms of the field enhancement associated with the concentrating effect due to the excitation of a surface polariton. The tenthousand-fold increase of the yield is associated with an additional effect: the near resonant excitation of a surface polariton at the sum frequency, giving rise to a substantial increase of the effective interaction length of the nonlinear optical process.

This technique has obvious applications, in particular in the area of SF spectroscopy of overlayers on top of metals, as has been recently demonstrated [23]. It combines well with the self-dispersive method for sum-frequency spectroscopy [10].

Acknowledgements. This work was supported by the Technology Foundation (STW) and the “Stichting voor Fundamenteel Onderzoek der Materie” (FOM). We highly appreciate the skilful assistance of the FELIX staff and gratefully acknowledge Dr. V.A. Yakovlev, Dr. L.A. Kuzik, Dr. E.V. Alieva and Dr. J.E. Petrov for their participation in the experiments and stimulating discussions.

References

1. Y.R. Shen: Nature **337**, 519 (1989)
2. K.B. Eisenthal: Annu. Rev. Phys. Chem. **43**, 627 (1992)
3. C.D. Bain: J. Chem. Soc. Faraday Trans. **91**, 1281 (1995)
4. P.-F. Brevet: *Surface Second Harmonic Generation* (Presses polytechniques et universitaires romande, Lausanne 1997)
5. D. Oepts, A.F.G. van der Meer, P.W. van Amersfoort: Infrared Phys. **36**, 297 (1995)
6. A. Peremans, P. Guyot-Sionnest, A. Tadjeddine, F. Glotin, J.-M. Ortega R. Prazères: Nucl. Instrum. Methods, Phys. Res. A **331**, 28 (1993)
7. M. Barmentlo, G.W. ’t Hooft, E.R. Eliel, E.W.M. van der Ham, Q.H.F. Vrehen, A.F.G. van der Meer, P.W. van Amersfoort: Phys. Rev. A **50**, R14 (1994)

8. A. Peremans, A. Tadjeddine: Phys. Rev. Lett. **73**, 3010 (1994)
9. E.R. Eliel, E.W.M. van der Ham, Q.H.F. Vrehen, G.W. 't Hooft, M. Barmentlo, J.M. Auerhammer, A.F.G. van der Meer, P.W. van Amersfoort: Appl. Phys. A **60**, 113 (1995)
10. E.W.M. van der Ham, Q.H.F. Vrehen, E.R. Eliel: Opt. Lett. **21**, 1448 (1996); E.W.M. van der Ham, Q.H.F. Vrehen, E.R. Eliel: Surf. Sci. **398**, 96 (1996)
11. R. Braun, B.D. Casson, C.D. Bain, E.W.M. van der Ham, Q.H.F. Vrehen, E.R. Eliel, A.M. Briggs, P.B. Davies: J. Chem. Phys., to appear (1999)
12. G.N. Zhizhin, M.A. Moskalova, E.V. Shomina, V.A. Yakovlev: *Surface Polaritons*, Chap. 3, ed. by V.M. Agranovich, D.L. Mills (North-Holland, Amsterdam 1982)
13. Y.R. Shen: Phys. Rep. **194**, 303 (1990)
14. S.R. Hatch, R.S. Polizotti, S. Dougal, P. Rabinowitz: Chem. Phys. Lett. **196**, 97 (1992)
15. C. Conboy, J. Daschbach, G. Richmond: J. Phys. Chem. **98**, 9688 (1994)
16. C. Conboy, M. Messmer, G. Richmond: J. Phys. Chem. **100**, 7617 (1996)
17. J. Löbau, K. Wolfrum: J. Opt. Soc. Am. B **14**, 2505 (1997)
18. E.V. Alieva, Y.E. Petrov, V.A. Yakovlev, E.R. Eliel, E.W.M. van der Ham, Q.H.F. Vrehen, A.F.G. van der Meer, V.A. Sychugov: JETP Lett. **66**, 609 (1997)
19. E.W.M. van der Ham, Q.H.F. Vrehen, E.R. Eliel, E.V. Alieva, L.A. Kuzik, V.A. Yakovlev, V.A. Sychugov: J. Opt. Soc. Am. B, to appear
20. E.V. Alieva, Y.E. Petrov, V.A. Yakovlev, E.R. Eliel, E.W.M. van der Ham, Q.H.F. Vrehen, V.A. Sychugov: to be published
21. A. Sommerfeld: Ann. Phys. (Leipzig) **4**, 665 (1909)
22. Y.R. Shen: *The Priciples of Nonlinear Optics* (Wiley, New York 1984)
23. E.V. Alieva, L.A. Kuzik, V.A. Yakovlev: Chem. Phys. Lett. **292**, 542 (1998)